Modulation of pulsatile GnRH dynamics across the ovarian cycle: the role of excitability within the arcuate kisspeptin network.

Margaritis Voliotis[1,*,†] , Xiao Feng Li[2,†], Ross De Burgh[2,†], Geffen Lass[2], Deyana Ivanova[2], Caitlin McIntyre[2],Kevin T. O'Byrne[2,*], Krasimira Tsaneva-Atanasova[1,*]
[1] Department of Mathematics and Living Systems Institute, College of Engineering, Mathematics and Physical Sciences, University of Exeter, Exeter, EX4 4QF, UK.
[2] Department of Women and Children's Health, School of Life Course Sciences, King's College London, London SE1 1UL, UK.
[†] These authors contributed equally to this work
[*] For correspondence: M.Voliotis@exeter.ac.uk, Kevin.O'Byrne@kcl.ac.uk, K.Tsaneva-Atanasova@exeter.ac.uk

Abstract

Pulsatile GnRH release is essential for normal reproductive function. Kisspeptin secreting neurons found in the arcuate nucleus, known as KNDy neurons for co-expressing neurokinin B, and dynorphin, drive pulsatile GnRH release. Furthermore, gonadal steroids regulate GnRH pulsatile dynamics across the ovarian cycle by altering KNDy neurons' signalling properties. However, the precise mechanism of regulation remains mostly unknown. Here we investigate these mechanisms using a combination of mathematical and in-vivo approaches. We find that optogenetic stimulation of KNDy neurons stimulates pulsatile GnRH/LH secretion in estrous mice but inhibits it in diestrous mice. Our mathematical modelling suggests that this differential effect is due to well-orchestrated changes in neuropeptide signalling and the excitability of the KNDy population controlled via glutamate signalling. Guided by model predictions, we show that blocking glutamate signalling in the arcuate nucleus in diestrous animals inhibits LH pulses, and that optic stimulation of the KNDy population mitigates this inhibition. In estrous mice, disruption of glutamate signalling inhibits pulses generated via sustained low-frequency optic stimulation of the KNDy population, supporting the idea that the level of network excitability is critical for pulse generation. Our results reconcile previous puzzling findings regarding the estradiol-dependent effect that several neuromodulators have on the GnRH pulse

generator dynamics. Therefore, we anticipate our model to be a cornerstone for a more quantitative understanding of the pathways via which gonadal steroids regulate GnRH secretion dynamics. Finally, our results could inform useful repurposing of drugs targeting the glutamate system in reproductive therapy.

Introduction

The dynamics of gonadotropin-releasing hormone (GnRH) secretion is critical for reproductive health. In female animals, GnRH secretion is tightly regulated across the ovarian cycle. Pulsatile secretion dominates most of the cycle, with frequency and amplitude modulated by the ovarian steroid feedback. Positive feedback from increasing estradiol levels triggers a preovulatory surge of GnRH/LH secretion (Christian and Moenter, 2010). Furthermore, there is ample evidence that ARC kisspeptin neurons are prime mediators of the ovarian steroid feedback on the pulsatile dynamics of GnRH/LH secretion (McQuillan et al., 2019), although the mechanisms remain unclear.

In-vitro studies have shown that gonadal steroids have a dramatic effect on the electrophysiology of ARC kisspeptin neurons. For instance, spontaneous firing activity of ARC kisspeptin neurons from castrated mice appears elevated compared to intact animals (Ruka et al., 2016) and estradiol replacement attenuates ARC kisspeptin neuron activity in gonadectomised animals (Ruka et al., 2016; Wang et al., 2018). Also gonadal steroids modulate the amplitude of LH pulses generated by intermittent optogenetic activation of ARC kisspeptin neurons (Han et al., 2015). More recently, fiber photometry data from female mice show that the ARC kisspeptin neuronal population (KNDy network) pulses at a relatively constant frequency throughout the ovarian cycle apart from the estrous phase where the frequency is dramatically reduced (McQuillan et al., 2019). This silencing effect is thought to be a direct consequence of the increasing progesterone levels in the circulation after ovulation has occurred (McQuillan et al., 2019). Furthermore, studies in the sheep indicate the silencing effect of progesterone is mediated through increased dynorphin signalling (Goodman et al., 2011; Moore et al., 2018), however this is less clear in mice where ovarian steroids have a negative effect on Dyn mRNA levels (Navarro et al., 2009).

Perplexing is also the differential effect of various neuromodulators on LH secretion depending on the gonadal steroid background. For instance, N-methyl-D-aspartate (NMDA) robustly inhibits LH pulses in the ovariectomized monkey whereas in the presence of estradiol this effect is reversed, and NMDA stimulates LH secretion (Reyes et al., 1990; Reyes et al., 1991).

Similar reversal of action on LH dynamics depending on the underlying ovarian steroid milieu has been also documented for other neurotransmitter and neuropeptides in other species (Kalra and Kalra, 1983; Brann and Mahesh, 1992; Arias et al., 1993; Bonavera et al., 1994; Scorticati et al., 2004) and highlights the complex mechanisms underlying the modulation the GnRH pulse generator by gonadal steroids.

Here, using mathematical modelling along with optogenetic stimulation of ARC kisspeptin neurons we embark to understand how the dynamics of the pulse generator are modulated across the ovarian cycle. Our mathematical model suggests that the level of excitability within the ARC kisspeptin network—the propensity of kisspeptin neurons to singal and activate each other—is one of the key parameters modulated in different stages of the cycles by gonadal steroids. Previous studies have shown that ARC kisspeptin neurons synapse on each other (Yip et al., 2015; Qiu et al., 2016) and because these neurons are mainly glutamatergic (Cravo et al., 2011; Qiu et al., 2011; Kelly et al., 2013; Wang et al., 2018), we hypothesise that population excitability should be enabled primarily via glutamatergic transmission. We test our predictions *in-vivo* and show that glutamatergic transmission is an important factor for the pulsatile behaviour of the KNDy network.

Materials and methods

Animals

Adult Kiss-Cre heterozygous transgenic female mice aged between 8-14 weeks, 25-30 g, were used for experiments (Yeo et al., 2016). Breeding pairs were obtained from the Department of Physiology, Development and Neuroscience, University of Cambridge, UK and mated in house at King's College London. Genotyping was performed using a multiplex PCR protocol for detection of heterozygosity for the Kiss-Cre or wild-type allele as previously described (Lass et al., 2020). Only mice with normal estrous cycles were used. Daily vaginal smears were performed for the detection of the estrous and diestrous stages of the ovarian cycle. Mice were singularly housed and provided with food (standard maintenance diet; Special Dietary Services, Wittam, UK) and water ad libitum while being kept under a 12:12 h light/dark cycle (lights on 0700 h) at 23 ± 2°C. All animal procedures performed were approved by the Animal Welfare and Ethical Review Body Committee at King’s College London and conducted in accordance with the UK Home Office Regulations.

Surgical procedures

96 Stereotaxic injection of AAV9-EF1-dflox-hChR2-(H134R)-mCherry-WPRE-hGH (4.35 x
97 1013 GC/ml; Penn Vector Core; University of Pennsylvania, PA, USA) for targeted expression
98 of channelrhodopsin (ChR2) in ARC kisspeptin neurons was done under aseptic conditions.
99 The mice were anaesthetised using ketamine (Vetalar, 100 mg/kg, i.p.; Pfizer, New York City,
100 NY, USA) and xylazine (Rompun, 10 mg/kg, i.p.; Bayer, Leverkusen, Germany). Kiss-Cre
101 female mice (n = 12) or wilt-type (n = 3) were secured in a Kopf Instruments motorized
102 stereotaxic frame (Kopf Instruments, Tujunga, CA, USA) and surgical procedures on the brain
103 were performed using a Robot Stereotaxy system (Neurostar, Tubingen, Germany). Stereotaxic
104 injection coordinates used to target the ARC were obtained from the mouse brain atlas of
105 Paxinos and Franklin (Paxinos and Franklin, 2004) (0.25 mm lateral, 1.94 mm posterior to
106 bregma and at a depth of 5.8 mm). A skin incision was made and a small hole was drilled in
107 the skull above the location of the ARC. A 2-µl Hamilton micro-syringe (Esslab, Essex, UK)
108 was attached to the robot stereotaxy and used to inject 0.3µl of the AAV-construct into the
109 ARC, unilaterally, at a rate of 100 nl/min. After the injection, the needle was left in position
110 for 5 min and then slowly lifted over 1 min. The same coordinates as the injection site were
111 then used to insert a fiber-optic cannula (200 µm, 0.39 NA, 1.25 mm ceramic ferrule; Thorlabs,
112 LTD, Ely, UK), however a depth of 5.78 mm was reached to ensure the fiber-optic cannula
113 was situated immediately above the injection site. Additionally, an intracerebroventricular
114 (ICV) fluid guide cannulae (26 gauge; Plastics One) targeting the lateral ventricle (coordinates:
115 1.1 mm lateral, 1.0 mm posterior to bregma and at a depth of 3.0 mm) was chronically
116 implanted. Dental cement (Superbond C&B kit Prestige Dental Products, Bradford UK) was
117 used to fix the cannulae in place and the skin incision was sutured. A one week recovery period
118 was given post-surgery. After this period, the mice were handled daily to acclimatize them to
119 the tail-tip blood sampling procedure (Steyn et al., 2013). Mice were left for 4 weeks to achieve
120 effective opsin expression before experimentation.

121 **Validation of AAV injection site and fibre optic and ICV cannula position**

122 Once experiments were completed, mice were given a lethal dose of ketamine and
123 transcardially perfused for 5 min with heparinized saline, followed by 10 min of ice-cold 4%
124 paraformaldehyde (PFA) in phosphate buffer, pH 7.4, for 15 min using a pump (Minipuls;
125 Gilson). Brain were collected immediately and post fixed at 4°C in 15% sucrose in 4% PFA
126 and left to sink. They were then transferred to 30% sucrose in PBS until they sank. The brains
127 were then snap-frozen on dry ice and stored at -80°C. Using a cryostat, every third coronal
128 brain section (30 µm) was collected between -1.34 mm to -2.70 mm from bregma and sections

129 were mounted on microscope slides, left to air-dry and cover slipped with ProLong Antifade
130 mounting medium (Molecular Probes, Inc, OR, USA). Verification and evaluation of the
131 injection site was performed using an Axioskop 2 Plus microscope equipped with axiovision
132 4.7 (Zeiss). One of 12 Kiss-Cre mice failed to show mCherry fluorescence in the ARC and was
133 excluded from the analysis.

134 **Experimental design and blood sampling for LH measurement.**

135 For measurement of LH pulsatility during optogenetic stimulation, the tip of the mouse's tail
136 was removed with a sterile scalpel for tail-tip blood sampling (Czieselsky et al., 2016). The
137 chronically implanted fiber-optic cannula was attached to a multimode fiber-optic rotary joint
138 patch cables (Thorlabs) via a ceramic mating sleeve. This allows for freedom of movement and
139 blue light delivery (473 nm wavelength) using a Grass SD9B stimulator controlled DPSS laser
140 (Laserglow Technologies) during optogenetic stimulation.
141 The experimental protocol involved an hour long acclimatisation period, followed by 2.5 h of
142 blood sampling, where 5 µl of blood was collected every 5 min. For estrous and diestrous mice,
143 optic stimulation was initiated after 1 h of control blood sampling and was sustained for 1.5 h
144 h. Optic stimulation was delivered as 5ms pulses of light at 5Hz with the laser intensity
145 measured at the tip of the fiber-optic patch cable set to 5mW. Additionally, in separate
146 experiments, diestrous mice were optically stimulated at 5 or 15 Hz for 2.5 h, that is entire
147 blood sampling period. Control mice (in estrus or diestrus) received no optic stimulation in, to
148 control for the effects of viral injections and surgical procedures. Wild-type mice
149 (estrus/disetrus???) received 5 Hz optic stimulation to verify that our optic stimulation protocol
150 had no undesirable effects on LH secretion.
151 Neuropharmacological manipulation of glutamatergic signalling was performed using a
152 combination of NMDA (AP5, Tocris, Abingdon, UK) and AMPA (CNQX, Alpha Aesar,
153 Heysham, UK) receptor antagonist treatment with or without simultaneous optogenetic
154 stimulation. The animals were prepared for optogenetic experimentation as described above
155 with additional preparation of the ICV injection cannula. Immediately after connection of the
156 fiber-optic cannula, the ICV injection cannula with extension tubing, preloaded with drug
157 solution (AP5 and CNQX dissolved in artificial CSF) or artificial CSF alone as control, was
158 inserted into the guide cannula. The extension tubing, reaching outside of the cage, was
159 connected to a 10 µl Hamilton syringe mounted in an automated pump (Harvard Apparatus) to
160 allow for remote micro-infusion without disturbing the animals during experimentation. After
161 a 55 min control blood sampling period, as described above, and 5 min before the onset of optic

162 stimulation, a bolus ICV injection of drug solution (12 nmol AP5 and 5 nmol CNQX in 2.3 μl)
163 was given over 5 min, followed by a continuous infusion (20 nmol AP5 and 10 nmol CNQX
164 in 5.6 μl) for the remaining 90 min of experimentation. Artificial CSF controls, with or without
165 optic stimulation, received the same ICV fluid regime. When no optic stimulation was applied
166 the same ICV administration and blood sampling regimen described was applied. Stimulation
167 and non-stimulation protocols were implemented in random order for Kiss-Cre mice.
168 The blood samples were snap-frozen on dry ice and stored at -80°C until processed. In-house
169 LH enzyme-linked immunosorbent assay (LH ELISA) similar to that described by Steyn et al.
170 was used for processing of the mouse blood samples (Steyn et al., 2013). The mouse LH
171 standard (AFP- 5306A; NIDDK-NHPP) was purchased from Harbor-UCLA along with the
172 primary antibody (polyclonal antibody, rabbit LH antiserum, AFP240580Rb; NIDDK-NHPP).
173 The secondary antibody (donkey anti-rabbit IgG polyclonal antibody [horseradish peroxidase];
174 NA934) was from VWR International. Validation of the LH ELISA was done in accordance
175 with the procedure described in Steyn et al. (Steyn et al., 2013) derived from protocols defined
176 by the International Union of Pure and Applied Chemistry. Serially diluted mLH standard
177 replicates were used to determine the linear detection range. Nonlinear regression analysis was
178 performed using serially diluted mLH standards of known concentration to create a standard
179 curve for interpolate the LH concentration in whole blood samples, as described in Voliotis et
180 al. (Voliotis et al., 2019). The intraassay and interassay variations were 4.6% and 10.2%,
181 respectively.

182 **LH pulse detection and statistical analysis.**

183 Dynpeak algorithm was used for the detection of LH pulses (Vidal et al., 2012). The differential
184 effect of optogenetic stimulation on LH pulsatility in estrus and diestrus was determined by
185 looking at the frequency of LH pulses. For mice in estrus and for the neuropharmacological
186 experiments, the mean ± SEM of LH pulses per hour were compared between the 60 min pre-
187 stimulation/drug delivery control period and subsequent 90 min stimulation period. For mice
188 in diestrus, the mean ± SEM of LH pulses per hour were compared between controls, 5 Hz and
189 15 Hz treatment groups, as optic stimulation was applied from the beginning of blood sample
190 period. No optic stimulation was applied to control animals, however the same time points
191 were compared. The frequency of LH pulses in the 90-min optic stimulation/drug delivery
192 period was also compared between treatment groups. One-way ANOVA followed by Dunnett's
193 test, $p < 0.05$, was used to determine statistical significance.

Mathematical model of the KNDy network.

We used a modified version of a mathematical model of the KNDy network previously presented in (Voliotis et al., 2019). Briefly, the model describes the ARC kisspeptin population in terms of three variables: $\bar{D}$, the average concentration of Dyn secreted by the population; $\bar{N}$, the average concentration of NKB secreted by the population; and $\bar{v}$, the average firing activity of the population, measured in spikes/min. The variables obey the following set of coupled ordinary differential equations (ODEs):

$$\frac{d\bar{D}}{dt} = f_D(\bar{v}) - d_D\bar{D}; \quad [1]$$

$$\frac{d\bar{N}}{dt} = f_N(\bar{v}, \bar{D}) - d_N\bar{N}; \quad [2]$$

$$\frac{d\bar{v}}{dt} = f_v(\bar{v}, \bar{N}) - d_v\bar{v}. \quad [3]$$

Parameters d_D, $d_N$and d_v control the characteristic timescale of each variable. The secretion rate of Dyn and NKB are given by:

$$f_D(\bar{v}) = k_{D,0}\frac{\bar{v}^{n_1}}{\bar{v}^{n_1} + K_{v,1}^{n_1}};$$

$$f_N(\bar{v}, \bar{D}) = k_N\frac{\bar{v}^{n_2}}{\bar{v}^{n_2} + K_{v,2}^{n_2}}\frac{K_D^{n_3}}{\bar{D}^{n_3} + K_D^{n_3}}.$$

In the equations above neuronal activity ($\bar{v}$) stimulates secretion of both neuropeptides, and Dyn represses NKB secretion. The maximum secretion rate for the two neuropeptides is controlled by parameters k_D and k_N and we refer to these parameters as the strength of Dyn and NKB singalling respectively. The effector levels at which saturation occurs are controlled via parameters $K_{v,1}$, $K_{v,2}$ and K_D. Here, we are interested in investigating the effect of network excitability on the dynamics therefore we modify the equation for the neuronal activity, $\bar{v}$, by setting:

$$f_v(\bar{v}, \bar{N}) = v_0\frac{1-\exp(-I)}{1+\exp(-I)}; I = I_0 + k_v\left(\frac{N^{n_4}}{N^{n_4}+K_N^{n_4}}\bar{v}\right),$$

where we have introduced parameter k_v capturing the strength of the synaptic connections between KNDy neurons in the ARC and which we will use a proxy for intrinsic network excitability. Furthermore, v_0 is the maximum rate at which the firing rate increases in response to synaptic inputs I. Note the stimulatory effect of NKB (which is secreted at the presynaptic terminal) on neuronal (Qiu et al., 2016) activity. Finally, parameter I_0 controls the basal

neuronal activity in the population, which could stem from synaptic noise or external inputs. Table 1 give the full list of model parameters.

Parameter inference

We used Approximate Bayesian Computation (ABC) based on sequential Monte Carlo (SMC) (Toni et al., 2009) to infer four key model parameters (Dyn signalling strength, k_D; NKB signalling strength, k_N; network excitability k_v; and basal activity, I_0) in the estrous and diestrous phase of the ovarian cycle. For this inference we used the average LH pulse frequency observed in four different settings: estrous animals without optic stimulation (F_E) and with 5Hz optic stimulation (F_{E+5Hz}); diestrus animals without optic stimulation (F_D) and with 5Hz optic stimulation (F_{D+5Hz}). Model simulations were generated in Matlab using function ode45 under the four different settings for 6000min and by calculating the frequencies after discarding the initial 1000min. The following discrepancy function was used to compare simulated data, $D^* = (F_E^*, F_{E+5Hz}^*, F_D^*, F_{D+5Hz}^*)$ to experimental data, $D = (F_E, F_{E+5Hz}, F_D, F_{D+5z})$:

$$d(D, D^*) = \max(\mathrm{abs}(D - D^*))$$

Furthermore, for the ABC SMC algorithm the size of the particle population was set to 500 and the algorithm was run for $T = 4$ populations with corresponding tolerance levels $\varepsilon_i = 10^{2-i}, i = 1, \dots, T$. The following prior distributions were used: $\log_{10}(k_D) \sim Uniform(-3,3)$, $\log_{10}(k_N) \sim Uniform(-3,3)$, $\log_{10}(k_v) \sim Uniform(-3,3)$., $\log_{10}(I_0) \sim Uniform(-3,3)$ All remaining parameters were fixed to values found in the literature (see Table 1). For each parameter an independent $\log_{10}$-normal perturbation kernel with variance 0.05 was used.

No	Parameter	Description	Value	Ref.
1	d_D	Dyn degradation rate	0.25 min^{-1}	(Voliotis et al., 2019)
2	d_N	NKB degradation rate	0.25 min^{-1}	(Voliotis et al., 2019)
3	d_v	Firing rate reset rate	10 min^{-1}	(Qiu et al., 2016)
4	k_D	Dyn singalling strength	inferred	
5	k_N	NKB signalling strength	inferred	(Ruka et al., 2016)
6	k_v	Network excitability	inferred	
7	v_0	Maximum rate of neuronal activity increase	30000 spikes min^{-2}	(Qiu et al., 2016)
8	K_D	Dyn IC_{50}	0.3 nM	(Yasuda et al., 1993)
9	K_N	NKB EC_{50}	32 nM	(Seabrook et al., 1995)
10	$K_{v,1}$	Firing rate for half-maximal Dyn secretion	1200 spikes min^{-1}	(Dutton and Dyball, 1979)
11	$K_{v,2}$	Firing rate for half-maximal NKB secretion	1200 spikes min^{-1}	(Dutton and Dyball, 1979)
12	I_0	Basal activity	inferred	
13	n_1, n_2, n_3, n_4	Hill coeffcients	2 (dimensionless)	fixed

Table 1. Model parameters values

Results

The dynamic response of the KNDy network to sustained, low-frequency optic stimulation is estrous cycle dependent.

To test whether and how sex steroids modulate the dynamical response of the KNDy network to sustained stimulation, ARC kisspeptin-expressing neurons were transduced with a Cre-dependent adeno-associated virus (AAV9-EF1-dflox-hChR2-(H134R)-mCherryWPRE-hGH) to express ChR2 (Fig. 1; see Materials and Methods) and were optogenetically stimulated at the estrous and the diestrous phase of the cycle, measuring LH pulse frequency as a readout of the system's dynamic response. Sustained, low-frequency optic stimulation was used to emulate elevated basal activity in ARC kisspeptin neurons or persistent stimulatory signals to the kisspepting population from other neuronal populations.

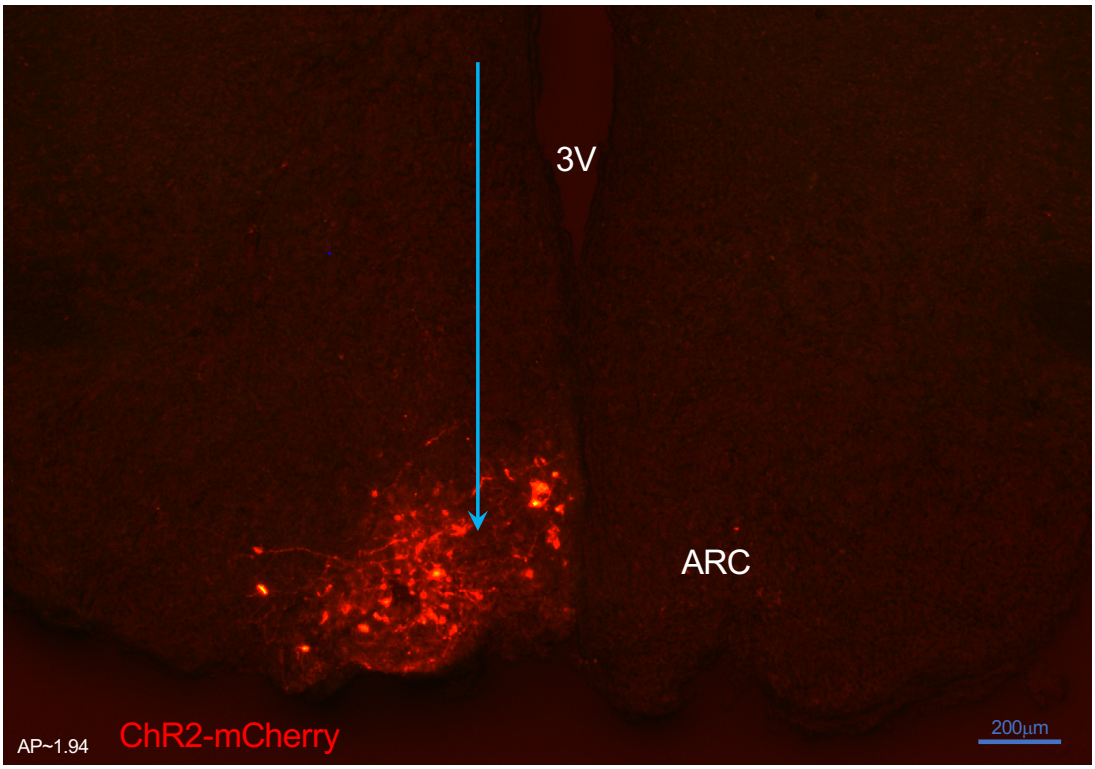

Figure 1. Expression of arcuate nucleus (ARC) kisspeptin neurones with ChR2-mCherry in Kiss-Cre mouse. Coronal section showing red mCherry fluorescence positive neurons in the ARC which indicates ChR2 receptor expressing kisspeptin neurones, following unilateral injection of AAV9.EF1.dflox.hChR2(H134R)-mCherry.WPRE.hGH into the ARC of Kiss-Cre mouse. The blue arrow shows the location of the injection site. Note the absence of mCherry fluorescence in the other side of ARC. 3V, Third ventricle.

262 In estrous mice, we find that sustained optogenetic stimulation of ARC kisspeptin neurons at
263 5Hz immediately triggers robust LH pulses at a frequency of 2.10 ± 0.24 pulses/hour (Fig. 2
264 A,C&E), which is in agreement with our previous findings (Voliotis et al., 2019) and highlights
265 how pulsatile dynanics can emerge as a population phenomemon without the need of an
266 intermittent activation signal (Strogatz, 2018). In diestrous mice, on the other hand, optogenetic
267 stimulation of ARC kisspeptin neurons at 5Hz leads to an apparent slowdown of LH pulse
268 frequency towards the end of the 1.5 h stimulation period (data not shown). To investigate the
269 response in diestrous mice in greater detail we revised our experimental protocol, removing the
270 control period and extending the stimulation period to 2.5 h. The revised protocol reveals a
271 decrease in LH pulse frequency to 0.64 ± 0.09 and 0.40 ± 0.13 pulses/hour for 5Hz and 15 Hz
272 optic stimulation respectively. albeit with a characteristic delay with 5 and 15 Hz optic
273 stimulation, respectively (Fig. 2 B,D&F).
274 Our data illustrate how natural variation of ovarian steroids across the cycle leads to qualitative
275 changes in the dynamical response of ARC kisspeptin neurons to optical stimulation. These
276 changes are most probably driven by the effect that gonadal steroids have on the intrinsic
277 electrophysiological properties of ARC kisspeptin neurons (Ruka et al., 2016) and the
278 neuromodulator signalling capacity within the KNDy network (Vanacker et al., 2017).

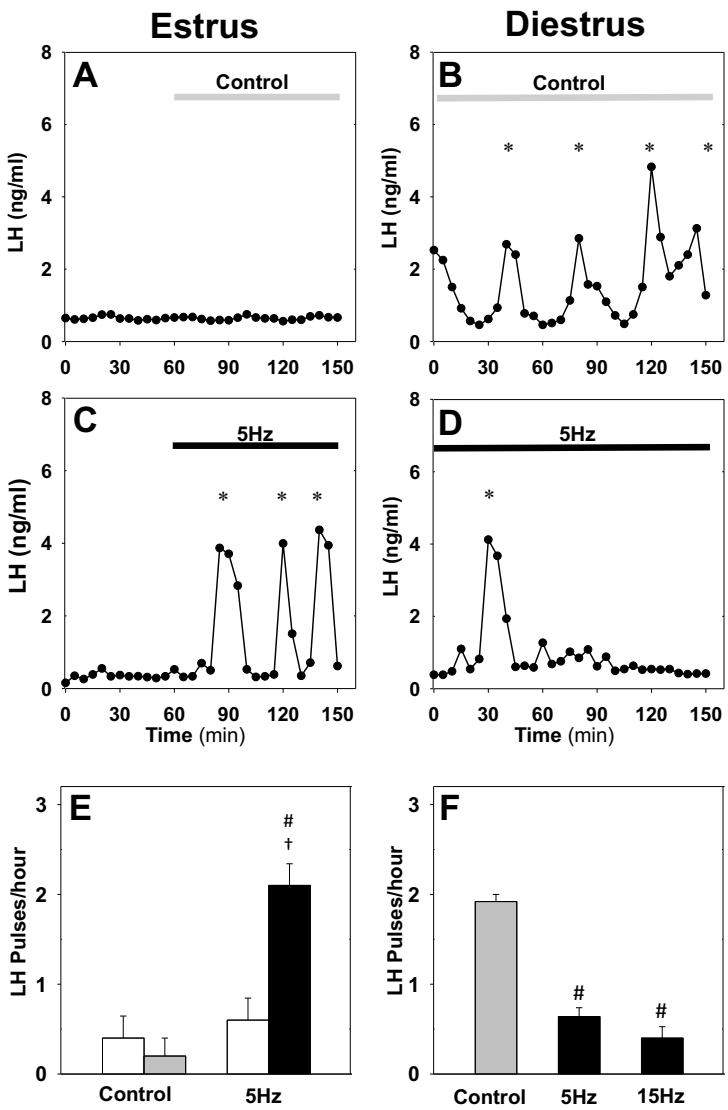

Figure 2. Differential effect of optic stimulation of ARC kisspeptin neurons in estrous and diestrous Kiss-Cre mice. (A-B) Representative examples showing LH secretion in response to no stimulation (grey bar) or sustained blue light (473 nm, 5-ms pulse width, black bar) activation of kisspeptin neurons at 5 Hz in estrous (C) and diestrous D) mice. (E) Summary showing mean ± SEM LH pulse frequency over the 60min control period (white bars) and over the subsequent stimulation period (black bar) in estrous mice. (F) Summary showing mean ± SEM LH pulse frequency in the control (grey bar) and stimulated (black bars) diestrous mice. *Denote LH pulses. $^{\#}P < 0.05$ vs control; $^{\dagger}P < 0.05$ vs pre-stimulation; n = 5-6 per group.

A mathematical model predicts key mechanisms modulating the behaviour of the KNDy pulse generator across the estrous cycle.

To understand the origin of the differential effect that optic stimulation of ARC kisspeptin neurons has across the ovarian cycle, we use our mathematical model of the KNDy network (Voliotis et al., 2019). The model describes the dynamical behaviour of ARC kisspeptin neurons using three dynamical variables: representing the levels of Dyn, NKB and neuronal

activity (Fig. 3 A). We postulate that gonadal steroids could potentially modulate the behaviour of the KNDy system across the cycle via acting on four key model parameters capturing the (i) level of Dyn signalling, (ii) level of NKB signalling, (iii) network excitability (i.e., propensity of neurons in the population to transmit signals to one another), and (iv) basal neuronal activity. Using the mean frequency data we observed experimentally in estrus and diestrus (with and without 5Hz optic stimulation; Fig. 2 E&F) and employing Bayesian inference techniques (see material and methods), we sample a population of estimates for these four parameters corresponding to diestrus and estrus. Inspection of the dynamical behaviour of the model, using the identified diestrous parameter values, reveals that in response to optic stimulation in diestrus pulsatile dynamics could die out gradually (i.e, there is a transient period before activity completely shuts down; see Fig. 3 B for an illustrative example), which is consistent with the delayed inhibition of LH pulses we observed experimentally in diestrous mice.

Next, we focus on how the four key parameters change between diestrus and estrus. We measure the change in each parameter using the log-ratio of its estrous to diestrous value, and calculate the covariance matrix of these log-ratios from our set of inferred parameter values. We find a positive (linear) correlation between changes in Dyn and NKB signalling strength, and negative (linear) correlation between changes in NKB signalling strength and network excitability (Fig. 3 C). That is, the model predicts that NKB signalling strength and network excitability are characterised by opposite (in direction) correlations during the transition from diestrus to estrus (one decreasing the other increasing; we note the model predicts that both combinations are possible), whereas NKB and Dyn signalling remain correlated in the same direction (ether increasing or decreasing; we note the model predicts that both combinations are possible). Finally, we apply Principal Component Analysis (PCA) to study the sensitivity of the system with respect to changes in the four parameters (Toni et al., 2009). We calculate the principal components in dataset with the inferred parameter changes. Principal components explaining small portions of the variance in the dataset (i.e., principal component with the smallest eigenvalue) correspond to parameter combinations to which the system dynamics are most sensitive (stiff parameter combinations). These combinations are the most critical in terms of regulation as small changes in the combined parameters result in significant shifts in the system's dynamics. Interestingly, the principal component capturing the smallest share of the variance is comprised of the parameters controlling NKB signalling, Dyn signalling and network excitability in approximately equal portions, and therefore the model predicts that co-

325 ordinated changes in these three parameters should be critical for the observed changes in
326 system dynamics between diestrus and estrus.
327 Taken together our theoretical findings suggest that network excitability in the KNDy network,
328 along with Dyn and NKB signalling, are crucial parameters of the GnRH pulse generator and
329 are tightly co-regulated across the reproductive cycle by the gonadal steroid milieu.
330

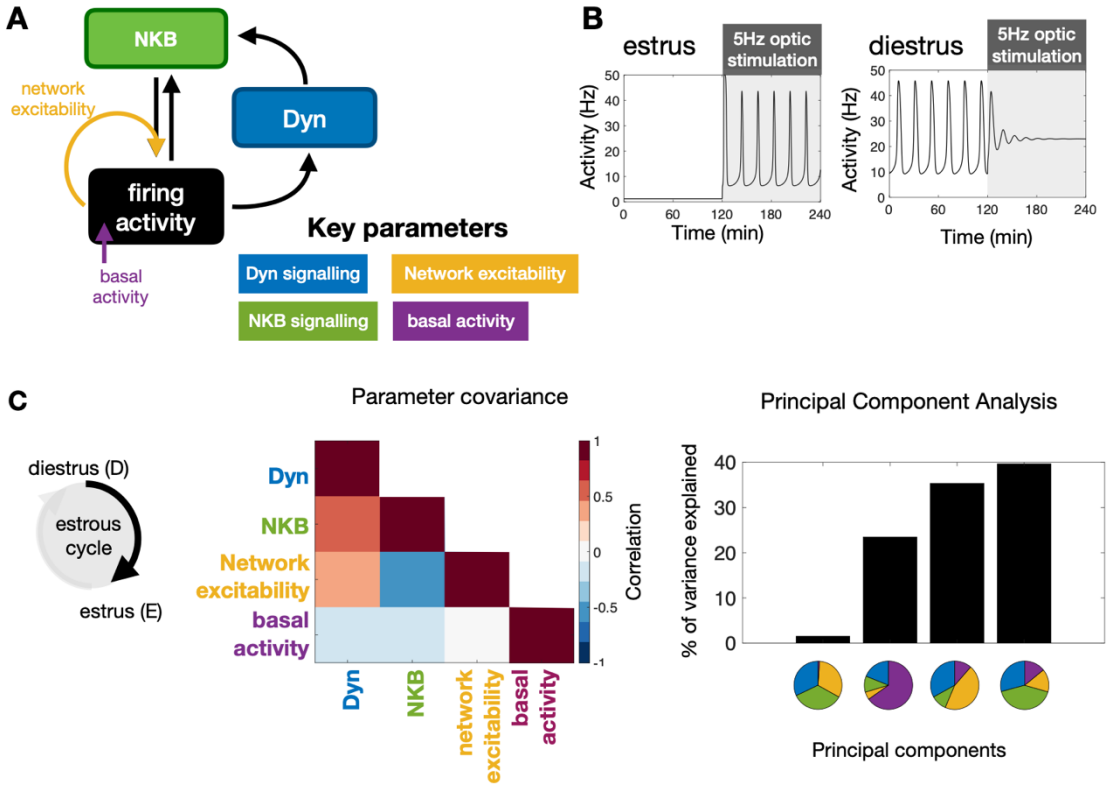

331
332 **Figure 3. Model predictions on the key mechanisms modulating the behaviour of the KNDy pulse generator**
333 **across the ovarian cycle**. (A) Schematic illustration of the coarse-grained model of the ARC KNDy population.
334 The model comprises three dynamical variables representing the average levels of Dyn and NKB secreted by the
335 population, and its average firing activity. We hypothesise that four key parameters modulate the behaviour of the
336 system across the ovarian cycle: (i) Dyn signalling strength; (ii) NKB signalling strength; (iii) network excitability
337 and (iv) basal neuronal activity. Estimates for the four parameters in estrus and diestrus are inferred from LH
338 pulse frequency data in estrus and diestrus animals; with or without 5Hz optic stimulation (Fig. 2 E&F) (B) System
339 response to low frequency stimulation during estrus and diestrus, using the maximum a-posteriori estimate of the
340 parameter values inferred from the frequency data. (C) Analysis of parameter changes across the cycle. For each
341 of the four parameter ($\theta^i; i = 1,2,3,4$) the diestrus-to-estrus change is defined as the log-ratio between the
342 corresponding parameter values, i.e., $\log_{10} {\theta^i_{\text{estrus}}}/{\theta^i_{\text{diestrus}}}$. Normalised covariance (correlation) matrix of
343 parameter changes reveals a strong negative correlation between changes in NKB signalling strength and network
344 excitability, and strong positive correlation between Dyn signalling strength and both NKB signalling and network

excitability. Principal component analysis produces a set of linearly uncorrelated eigen-parameters explaining the variance of the inferred parameter values (posterior distribution). These eigen-parameters are linear weighted combinations of the initial parameters and are visualised as pie charts. The eigen-parameter explaining the least of the variance in the posterior distribution corresponds to the stiffest parameter combination to which the system is most sensitive.

Glutamatergic transmission in the KNDy population is critical for LH pulsatility

The model predicts that excitability in the KNDy network (i.e., the efficacy of ARC kisspeptin neurons to signal and excite each other) is one of the critical parameters controlling the dynamic behaviour of the system across the ovarian cycle. As ARC kisspeptin neurons are mainly glutamatergic (Cravo et al., 2011), we hypothesise that network excitability should be enabled primarily via glutamatergic transmission. We therefore set out to test how disrupting signalling via glutamate receptors impacts LH pulsatility.

First, using Kiss-Cre estrous mice we test whether glutamatergic transmission is necessary for the optogentic induction of LH pulses. We drive the ARC kisspeptin population using sustained, low-frequency optic stimulation (5 Hz) in the presence of the combined NMDA and AMPA receptor antagonists (AP5 and CNQX, respectively). We find that blocking signalling via glutamate receptors inhibits the capacity of optic stimulation to generate and sustain pulsatile LH secretion (Fig. 4 A,B&D). The combined AP5 and CNQX in the absence of optic stimulation had no effect (Fig. 4 C&D).

Next, we test whether glutamatergic transmission is critical for the endogenous LH pulses observed in diestrus. Treatment of diestrous mice with the combined NMDA and AMPA receptor antagonists resulted in a significant reduction of LH pulse frequency from 2.50 ± 0.29 to 0.45 ± 0.15 pulses/hour (Fig. 5 B&D), confirming that the glutamatergic transmission is indeed critical for pulsatility. Moreover, combining NMDA and AMPA receptor antagonist treatment with low frequency optic stimulation (5 Hz) partially restored LH pulsatility to 1.58 ± 0.17 pulses/hour (Fig. 5 C&D), suggesting low network excitability could be offset by exogenous inputs or elevated basal activity and highlighting the complex regulatory interactions that are underpinning pulsatile GnRH secretion.

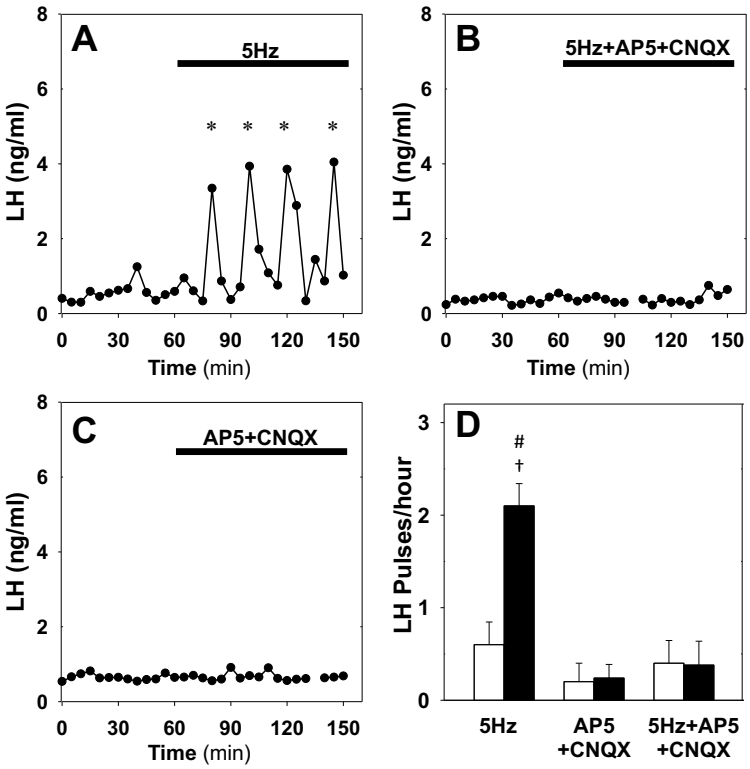

Figure 4. Effect of NMDA+AMPA receptor antagonists on pulsatile LH secretion in estrus. Representative examples showing LH secretion in estrous mice in response to optic stimulation (5Hz blue light, 473 nm, 5-ms pulse width) (A) and optic stimulation combined with the NMDA+AMPA receptor antagonist (bolus ICV injection [12 nmol AP5 + 5 nmol CNQX] over 5 min, followed by a continuous infusion [20 nmol AP5 and 10 nmol CNQX] for the remaining 90 min) treatment (B). NMDA+AMPA receptor antagonist alone had no effect (C). (D) Summary showing mean ± SEM LH pulse frequency over the 60min non-stimulatory period (white bars) and over the subsequent 90 min stimulation period or appropriate non-stimulatory period in presence of. NMDA+AMPA receptor antagonist alone (black bar) in diestrous mice. *Denote LH pulses. $^{\dagger}P < 0.05$ vs pre-stimulation. $^{\#}P < 0.05$ compared to antagonist treatment groups; n = 5-6 per group.

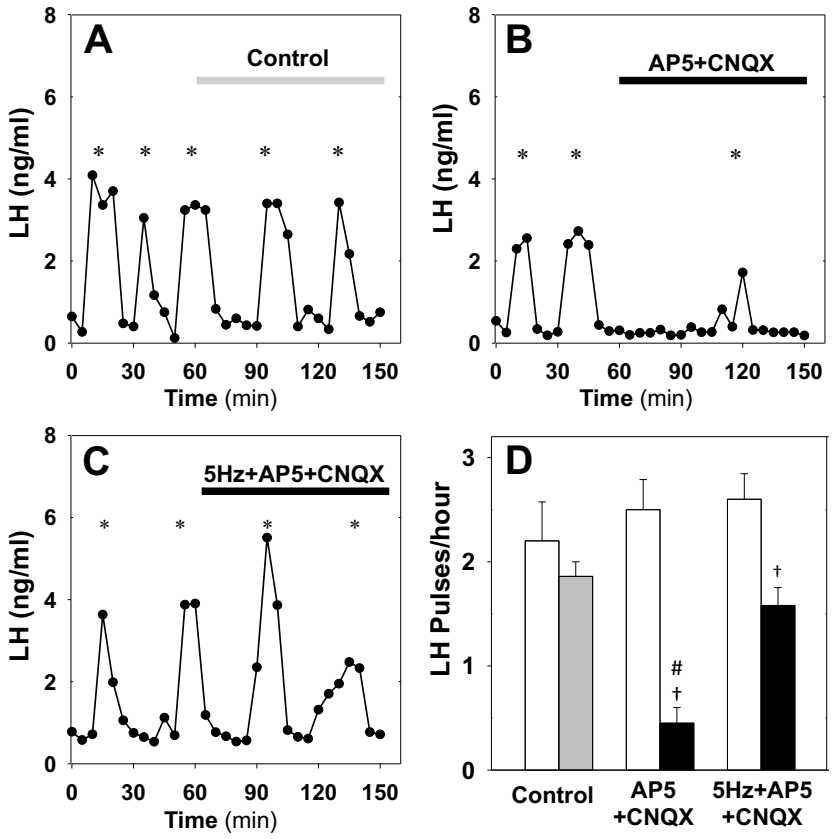

Figure 5. Effect of NMDA+AMPA receptor antagonists on pulsatile LH secretion in diestrus. Representative examples showing pulsatile LH secretion in response to ICV administration of aCSF as control (A), treatment with NMDA+AMPA receptor antagonists (AP5+CNQX: bolus ICV injection [12 nmol AP5 + 5 nmol CNQX] over 5 min, followed by a continuous infusion [20 nmol AP5 and 10 nmol CNQX] for the remaining 90 min) (B) and combined NMDA/AMPA receptor antagonist treatment and sustained optic stimulation (blue light 473 nm, 5-ms pulse width) at 5Hz (C). (D) Summary showing mean ± SEM LH pulse frequency over the 60min non-stimulatory period (white bars) and over the subsequent 90 min stimulation period in control mice (grey bar) and mice receiving treatment (black bar). *Denote LH pulses. $^{\dagger}P < 0.05$ vs pre-stimulation. $^{\#}P < 0.05$ compared to 5 Hz stimulation plus antagonist treatment and aCSF control groups; n = 5-6 per group.

Discussion

Using optogenetics we probed the dynamic response of the GnRH pulse generator at different stages of the ovarian cycle. Previous studies have shown how the pulsatile activity generated by the kisspeptin neuronal network is modulated across the estrous cycle (Han et al., 2015; McQuillan et al., 2019). Our data show that the stage of the cycle has also a profound effect on the dynamical response of the kisspeptin population to sustained, low frequency optic stimulation: with stimulation during estrus accelerating LH pulses, while stimulation during the diestrus phase slowing them down. This is suggestive of a critical role of the gonadal state

401 in modulating the dynamical response of the KNDy network to small changes in basal activity
402 of ARC kisspeptin neurons or in how the population processes external neuronal inputs.

403 Using our mathematical model of the system we gained insight into possible mechanisms via
404 which gonadal steroids modulate the dynamic behaviour of the GnRH pulse generator. Based
405 on the LH pulse frequency observed in estrous and diestrous animals under no optic stimulation
406 or with 5Hz optic stimulations, the model predicted that network excitability is an important
407 parameter of the system, which could be modulated at different stages of the ovarian cycle.
408 Importantly, KNDy network excitability is most probably co-regulated with parameters
409 controlling the strength of Dyn and NKB signalling as the system transitions between the
410 different phases of the ovarian cycle. In particular, our analysis suggests strong negative
411 correlation between changes in NKB signalling strength and changes in network excitability
412 and strong positive correlation in changes between NKB and Dyn signalling. Interestingly
413 these finding are in line with recent transcriptomic data showing that treatment of
414 ovariectomised mice with estradiol reduced expression of NKB and Dyn but increased
415 expression of glutamate transporters (vGlut2) leading to increased glutamate
416 neurotransmission and neuronal excitability (Qiu et al., 2018).

417 The effect of cycle stage on the LH response to sustained optogenetic stimulation is reminiscent
418 of the well documented effect that gonadal steroids have on LH response to various excitatory
419 neurotransmitters and neuropeptides (e.g., NMDA). For instance, investigations in the female
420 monkey revealed an unexplained inhibition of LH in OVX animals following treatment with
421 NMDA, in contrast with the excitatory action of NMDA on LH secretion in the presence of
422 ovarian steroids (Reyes et al., 1990; Reyes et al., 1991). Similar reversal of action on LH
423 dynamics depending on the underlying ovarian steroid milieu has been documented for various
424 other neurotransmitters and NKB receptor agonists (Kalra and Kalra, 1983; Scorticati et al.,
425 2004). Our mathematical model supports that ovarian steroids change key parameters of the
426 KNDy network, which control the dynamic behaviour of the system and its response to
427 perturbations. As an illustration, Fig. 6 shows how the dynamic behaviour of the model
428 depends on network excitability and NKB signalling. Since these parameters are governed by
429 gonadal steroids (Qiu et al., 2018; Wang et al., 2018), it is expected that the underlying steroid
430 milieu will also modulate the effect of perturbations on the dynamics of the system. For
431 instance, the effect of stimulating NKB signalling (e.g., via administration of NK3 receptor
432 agonists) or network excitability (e.g., via NMDA administration) could result in inhibition of

433 the pulse generator if the system is already located closer to the right boundary of the pulsatile
434 dynamics region (e.g., point B in Fig. 6). Such points correspond to states with high pulse
435 generator activity similar to pulse generator dynamics observed in many animal models after
436 gonadectomy (Reyes et al., 1990; Kinsey-Jones et al., 2012). In contrast, similar perturbations
437 but from a different point in the parameter space, lying closer to the left edge of the pulsatile
438 region (e.g., point A in Fig. 6), could result in stimulation of the pulse generator (higher
439 frequency). This illustrative example also highlights that it is the actual continuous levels of
440 the gonadal steroids modulating the response of the pulse generator to perturbations rather than
441 their mere presence or absence. Therefore, the underlying steroid levels could explain
442 seemingly incompatible findings regarding the effect of NKB receptor agonism on LH
443 secretion: ranging from stimulation (Navarro et al., 2011) or inhibition (Sandoval-Guzman and
444 Rance, 2004; Kinsey-Jones et al., 2012) to no effects (Navarro et al., 2009) in rodents.

445

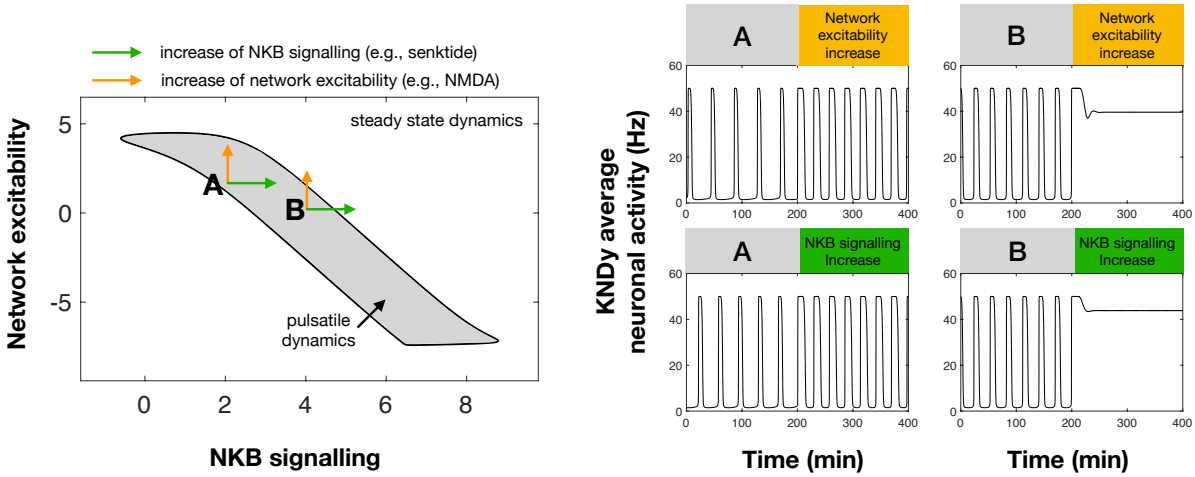

446
447 **Figure 6. Differential effect of perturbations on the dynamics of the pulse generator.** Two-parameter (NKB
448 signalling and Network excit ability) bifurcation diagram showing the region in the parameter space for which the
449 system exhibits pulsatile dynamics (grey area). Two points (denoted by A and B) illustrate how an increase in NKB
450 signalling or network excitability could have a differential effect on the dynamics of the system. For point A an
451 increase in network excitability or NKB signalling could lead to an increase in the frequency and width of pulses.
452 However, for point B a similar increase leads to pulse inhibition and steady state system dynamics.

453 Based on our model predictions regarding the importance of network excitability, we set out
454 to uncover the role of this parameter on the dynamic response of the network in-vivo. We
455 hypothesised that network excitability should critically depend on the levels of glutamate
456 signalling as ARC kisspeptin neurons are known to synapse one another (Yip et al., 2015; Qiu
457 et al., 2016) and are primarily glutamatergic (Cravo et al., 2011; Qiu et al., 2011; Kelly et al.,
458 2013; Wang et al., 2018). Therefore, we used glutamate receptor (NMDA and AMPA)
459 antagonists to inhibit excitability in the KNDy network. ICV delivery of these antagonists

leaves open the possibility of interfering with the glutamatergic transmission of other neuronal population to the KNDY population. Nevertheless, the effect of blocking these exogenous inputs should be secondary to the effect of blocking signalling between kisspeptin neurons. Indeed, our results suggested a critical role for glutamate in enabling the population to synchronise and pulse in unison. In diestrus animals blocking glutamate receptors (NMDA and AMPA) inhibited LH pulses that were then rescued via low frequency optogenetic stimulation of kisspeptin neurons. Furthermore, in estrus animals, NMDA and AMPA receptor antagonism inhibited the induction of LH pulses via optic stimulation. These experimental findings highlight the complex fine-balanced mechanisms underlying pulse generation by the KNDy network. In particular, limited glutamatergic signalling within the KNDy population blocks LH pulsatility but this can be mitigated by elevated basal neuronal activity. Similarly, increased basal neuronal activity can induce pulse generation but this effect can be negated by decreased glutamatergic signalling within the neuronal population. Pulse generation is therefore an emergent property of the KNDy network depending both on intrinsic, single neuron properties such as basal activity but also on how the neurons signal and communicate with each other.

Acknowledgments: The authors gratefully acknowledge the financial support of the EPSRC via grant EP/N014391/1 (KTA and MV), and BBSRCH via grants BB/S000550/1 and BB/S001255/1 (KTA, KOB, MV, XFL).

References

Arias P, Jarry H, Leonhardt S, Moguilevsky JA, Wuttke W (1993) Estradiol modulates the LH release response to N-methyl-D-aspartate in adult female rats: studies on hypothalamic luteinizing hormone-releasing hormone and neurotransmitter release. Neuroendocrinology 57:710-715.

Bonavera JJ, Sahu A, Kalra SP, Kalra PS (1994) The hypothalamic peptides, beta-endorphin, neuropeptide K and interleukin-1 beta, and the opiate morphine, enhance the excitatory amino acid-induced LH release under the influence of gonadal steroids. J Neuroendocrinol 6:557-564.

Brann DW, Mahesh VB (1992) Excitatory amino acid regulation of gonadotropin secretion: modulation by steroid hormones. J Steroid Biochem Mol Biol 41:847-850.

Christian CA, Moenter SM (2010) The neurobiology of preovulatory and estradiol-induced gonadotropin-releasing hormone surges. Endocr Rev 31:544-577.

Cravo RM, Margatho LO, Osborne-Lawrence S, Donato J, Jr., Atkin S, Bookout AL, Rovinsky S, Frazao R, Lee CE, Gautron L, Zigman JM, Elias CF (2011) Characterization of Kiss1 neurons using transgenic mouse models. Neuroscience 173:37-56.

Czieselsky K, Prescott M, Porteous R, Campos P, Clarkson J, Steyn FJ, Campbell RE, Herbison AE (2016) Pulse and Surge Profiles of Luteinizing Hormone Secretion in the Mouse. Endocrinology 157:4794-4802.

499 Dutton A, Dyball RE (1979) Phasic firing enhances vasopressin release from the rat
500 neurohypophysis. J Physiol 290:433-440.
501 Goodman RL, Holaskova I, Nestor CC, Connors JM, Billings HJ, Valent M, Lehman MN,
502 Hileman SM (2011) Evidence that the arcuate nucleus is an important site of
503 progesterone negative feedback in the ewe. Endocrinology 152:3451-3460.
504 Han SY, McLennan T, Czieselsky K, Herbison AE (2015) Selective optogenetic activation of
505 arcuate kisspeptin neurons generates pulsatile luteinizing hormone secretion. Proc Natl
506 Acad Sci U S A 112:13109-13114.
507 Kalra SP, Kalra PS (1983) Neural regulation of luteinizing hormone secretion in the rat. Endocr
508 Rev 4:311-351.
509 Kelly MJ, Zhang C, Qiu J, Ronnekleiv OK (2013) Pacemaking kisspeptin neurons. Exp Physiol
510 98:1535-1543.
511 Kinsey-Jones JS, Grachev P, Li XF, Lin YS, Milligan SR, Lightman SL, O'Byrne KT (2012)
512 The inhibitory effects of neurokinin B on GnRH pulse generator frequency in the
513 female rat. Endocrinology 153:307-315.
514 Lass G, Li XF, de Burgh RA, He W, Kang Y, Hwa-Yeo S, Sinnett-Smith LC, Manchishi SM,
515 Colledge WH, Lightman SL, O'Byrne KT (2020) Optogenetic stimulation of kisspeptin
516 neurones within the posterodorsal medial amygdala increases luteinising hormone
517 pulse frequency in female mice. J Neuroendocrinol 32:e12823.
518 McQuillan HJ, Han SY, Cheong I, Herbison AE (2019) GnRH Pulse Generator Activity Across
519 the Estrous Cycle of Female Mice. Endocrinology 160:1480-1491.
520 Moore AM, Coolen LM, Porter DT, Goodman RL, Lehman MN (2018) KNDy Cells Revisited.
521 Endocrinology 159:3219-3234.
522 Navarro VM, Gottsch ML, Chavkin C, Okamura H, Clifton DK, Steiner RA (2009) Regulation
523 of gonadotropin-releasing hormone secretion by kisspeptin/dynorphin/neurokinin B
524 neurons in the arcuate nucleus of the mouse. J Neurosci 29:11859-11866.
525 Navarro VM, Castellano JM, McConkey SM, Pineda R, Ruiz-Pino F, Pinilla L, Clifton DK,
526 Tena-Sempere M, Steiner RA (2011) Interactions between kisspeptin and neurokinin B
527 in the control of GnRH secretion in the female rat. Am J Physiol Endocrinol Metab
528 300:E202-210.
529 Paxinos G, Franklin KBJ (2004) The Mouse Brain in Stereotaxic Coordinates, 2nd Edition:
530 Elsevier Academic Press.
531 Qiu J, Fang Y, Bosch MA, Ronnekleiv OK, Kelly MJ (2011) Guinea pig kisspeptin neurons
532 are depolarized by leptin via activation of TRPC channels. Endocrinology 152:1503-
533 1514.
534 Qiu J, Nestor CC, Zhang C, Padilla SL, Palmiter RD, Kelly MJ, Ronnekleiv OK (2016) High-
535 frequency stimulation-induced peptide release synchronizes arcuate kisspeptin neurons
536 and excites GnRH neurons. Elife 5:e16246-e16246.
537 Qiu J, Rivera HM, Bosch MA, Padilla SL, Stincic TL, Palmiter RD, Kelly MJ, Ronnekleiv OK
538 (2018) Estrogenic-dependent glutamatergic neurotransmission from kisspeptin neurons
539 governs feeding circuits in females. Elife 7.
540 Reyes A, Luckhaus J, Ferin M (1990) Unexpected inhibitory action of N-methyl-D,L-aspartate
541 or luteinizing hormone release in adult ovariectomized rhesus monkeys: a role of the
542 hypothalamic-adrenal axis. Endocrinology 127:724-729.
543 Reyes A, Xia LN, Ferin M (1991) Modulation of the effects of N-methyl-D,L-aspartate on
544 luteinizing hormone by the ovarian steroids in the adult rhesus monkey.
545 Neuroendocrinology 54:405-411.
546 Ruka KA, Burger LL, Moenter SM (2016) Both Estrogen and Androgen Modify the Response
547 to Activation of Neurokinin-3 and kappa-Opioid Receptors in Arcuate Kisspeptin
548 Neurons From Male Mice. Endocrinology 157:752-763.

549 Sandoval-Guzman T, Rance NE (2004) Central injection of senktide, an NK3 receptor agonist,
550 or neuropeptide Y inhibits LH secretion and induces different patterns of Fos
551 expression in the rat hypothalamus. Brain Res 1026:307-312.
552 Scorticati C, Fernandez-Solari J, De Laurentiis A, Mohn C, Prestifilippo JP, Lasaga M,
553 Seilicovich A, Billi S, Franchi A, McCann SM, Rettori V (2004) The inhibitory effect
554 of anandamide on luteinizing hormone-releasing hormone secretion is reversed by
555 estrogen. Proc Natl Acad Sci U S A 101:11891-11896.
556 Seabrook GR, Bowery BJ, Hill RG (1995) Pharmacology of tachykinin receptors on neurones
557 in the ventral tegmental area of rat brain slices. Eur J Pharmacol 273:113-119.
558 Steyn FJ, Wan Y, Clarkson J, Veldhuis JD, Herbison AE, Chen C (2013) Development of a
559 methodology for and assessment of pulsatile luteinizing hormone secretion in juvenile
560 and adult male mice. Endocrinology 154:4939-4945.
561 Strogatz SH (2018) Nonlinear dynamics and chaos with student solutions manual: With
562 applications to physics, biology, chemistry, and engineering: CRC press.
563 Toni T, Welch D, Strelkowa N, Ipsen A, Stumpf MP (2009) Approximate Bayesian
564 computation scheme for parameter inference and model selection in dynamical
565 systems. J R Soc Interface 6:187-202.
566 Vanacker C, Moya MR, DeFazio RA, Johnson ML, Moenter SM (2017) Long-Term
567 Recordings of Arcuate Nucleus Kisspeptin Neurons Reveal Patterned Activity That Is
568 Modulated by Gonadal Steroids in Male Mice. Endocrinology 158:3553-3564.
569 Vidal A, Zhang Q, Medigue C, Fabre S, Clement F (2012) DynPeak: an algorithm for pulse
570 detection and frequency analysis in hormonal time series. PLoS One 7:e39001.
571 Voliotis M, Li XF, De Burgh R, Lass G, Lightman SL, O'Byrne KT, Tsaneva-Atanasova K
572 (2019) The Origin of GnRH Pulse Generation: An Integrative Mathematical-
573 Experimental Approach. J Neurosci 39:9738-9747.
574 Wang L, Burger LL, Greenwald-Yarnell ML, Myers MG, Jr., Moenter SM (2018)
575 Glutamatergic Transmission to Hypothalamic Kisspeptin Neurons Is Differentially
576 Regulated by Estradiol through Estrogen Receptor alpha in Adult Female Mice. J
577 Neurosci 38:1061-1072.
578 Yasuda K, Raynor K, Kong H, Breder CD, Takeda J, Reisine T, Bell GI (1993) Cloning and
579 functional comparison of kappa and delta opioid receptors from mouse brain. Proc Natl
580 Acad Sci U S A 90:6736-6740.
581 Yeo SH, Kyle V, Morris PG, Jackman S, Sinnett-Smith LC, Schacker M, Chen C, Colledge
582 WH (2016) Visualisation of Kiss1 Neurone Distribution Using a Kiss1-CRE
583 Transgenic Mouse. J Neuroendocrinol 28.
584 Yip SH, Boehm U, Herbison AE, Campbell RE (2015) Conditional Viral Tract Tracing
585 Delineates the Projections of the Distinct Kisspeptin Neuron Populations to
586 Gonadotropin-Releasing Hormone (GnRH) Neurons in the Mouse. Endocrinology
587 156:2582-2594.
588